

## Loaded waveguide measurements of plastic explosives at V-band

Zachary J. Landicini,<sup>a</sup> Jeffrey Barber,<sup>b</sup> James C. Weatherall,<sup>b,\*</sup> Duane C. Karns,<sup>b</sup> Peter R. Smith,<sup>c</sup> Joaquín Aparicio-Bolaño,<sup>a</sup> and Wendy Ruiz<sup>a</sup>

<sup>a</sup>Battelle Memorial Institute, Egg Harbor Township, New Jersey, United States

<sup>b</sup>William J. Hughes Technical Center, U.S. Department of Homeland Security, Science and Technology Directorate, Atlantic City International Airport, New Jersey, United States

<sup>c</sup>MAG Aerospace, Tinton Falls, New Jersey, United States

**ABSTRACT.** Dielectric measurements of plastic explosives using a loaded waveguide technique via vector network analyzer and banded millimeter wave extender modules operating at V-band (50 to 75 GHz) are performed. A portion of an explosive sample is inserted into a waveguide shim 2 mm in length and trimmed flush with the faces of the shim. Two-port S-parameter measurements are conducted on the explosive; the empty shim is similarly characterized. Using standard waveguide equations and the measured length of the shim, the complex S-parameter data obtained with the filled shim is optimized to four free parameters—complex permittivity and distance offsets for the two sample faces relative to the calibration planes. Permittivity data obtained from measurements of the plastic explosives C-4, Primasheet 1000, Primasheet 2000 and Semtex 10 are presented. Results obtained for C-4 and Primasheet 1000 are comparable to other data in the literature, and the data on Primasheet 2000 and Semtex 10 are the first known published permittivity values in this range. Excellent agreement between the experiment and the fit is obtained using a constant permittivity across the waveguide band, indicating that dispersion is not significant for these materials.

© The Authors. Published by SPIE under a Creative Commons Attribution 4.0 International License. Distribution or reproduction of this work in whole or in part requires full attribution of the original publication, including its DOI. [DOI: [10.1117/1.JRS.18.014501](https://doi.org/10.1117/1.JRS.18.014501)]

**Keywords:** millimeter wave; dielectric measurement; reflection coefficient; explosives detection; millimeter wave

Paper 230556G received Oct. 16, 2023; revised Nov. 30, 2023; accepted Dec. 6, 2023; published Dec. 29, 2023.

### 1 Introduction

The Transportation Security Laboratory, operated by the U.S. Department of Homeland Security's Science and Technology Directorate, performs dielectric measurements on explosives for the purpose of designing simulants to support the test and evaluation of advanced imaging technology (AIT)<sup>1–5</sup> systems deployed for explosives detection. The development of AIT systems, such as the Rohde and Schwarz QPS imaging systems,<sup>6–9</sup> operating in the range of 70 to 80 GHz necessitates that the dielectric properties of explosives be measured at higher frequencies. Past studies have used techniques such as resonant cavities<sup>1</sup> and free space methods<sup>10</sup> to characterize these materials. Going to higher frequencies using resonant cavities has been challenging. As the frequency increases, the wavelength gets smaller, and the resonant cavities must decrease in size with the wavelength. As a result, repeatability of the polyethylene fixtures used for these measurements have been poor as the wavelength approaches machining tolerances. Free space methods, although simple, require significant sample sizes (4 inches in diameter) and a

\*Address all correspondence to James C. Weatherall, [james.weatherall@st.dhs.gov](mailto:james.weatherall@st.dhs.gov)

uniform thickness. Getting uniform samples of a sticky putty substance, such as C-4, is challenging, and the size significantly increases the safety hazards.

The loaded waveguide technique for permittivity measurements has been used to characterize solid materials, such as plastics,<sup>11</sup> glass,<sup>12</sup> and concrete,<sup>13</sup> as well as liquid and granular materials.<sup>14,15</sup> The use of waveguides for permittivity measurements has also been adopted as an ASTM international standard method.<sup>16</sup> When coupled with the aforementioned challenges to using other techniques, the loaded waveguide technique is particularly attractive for semi-solid explosives. The loaded waveguide can be filled by hand, and the volume of the sample can be reduced from the order of 100 milliliters (free space method) to tens of microliters, dramatically increasing the safety of the measurements.

This report documents the dielectric characterization of the explosives C-4, Primasheet 1000, Primasheet 2000, and Semtex 10 using a V-band (50 to 75 GHz) loaded waveguide technique. The theory of this technique and adaptations made to account for the nature of the sample are presented. Data obtained on the empty waveguide fixture are used to both determine the length of the sample holder and ensure that the fixture is in agreement with waveguide theory. Permittivity results of the plastic explosives are presented and discussed relative to other values available in the literature.

## 2 Methods and Techniques

Figure 1 displays a diagram of the loaded waveguide method used in this work. The theory of electromagnetic propagation in a rectangular waveguide and its interaction with a dielectric sample are well understood.<sup>11,17</sup> Briefly, the scattering parameters (S-parameters) obtained from a measurement of a sample are given as

$$S_{11} = R_1^2 \Gamma \frac{(1 - T^2)}{1 - \Gamma^2 T^2}, \quad (1)$$

$$S_{22} = R_2^2 \Gamma \frac{(1 - T^2)}{1 - \Gamma^2 T^2}, \quad (2)$$

$$S_{21} = S_{12} = R_1 R_2 T \frac{(1 - \Gamma^2)}{1 - \Gamma^2 T^2}, \quad (3)$$

where  $\Gamma$  is the reflection coefficient of an infinite sample,  $T$  is the propagation factor, and  $R_1$  and  $R_2$  are the calibration plane transformation factors. These are further defined as

$$\Gamma = \frac{\gamma_0 - \gamma}{\gamma_0 + \gamma}, \quad (4)$$

$$T = \exp(-\gamma L_{\text{sample}}), \quad (5)$$

$$\gamma = \sqrt{\kappa_c^2 - \epsilon_r \kappa_0^2}, \quad (6)$$

$$\gamma_0 = \sqrt{\kappa_c^2 - \kappa_0^2}, \quad (7)$$

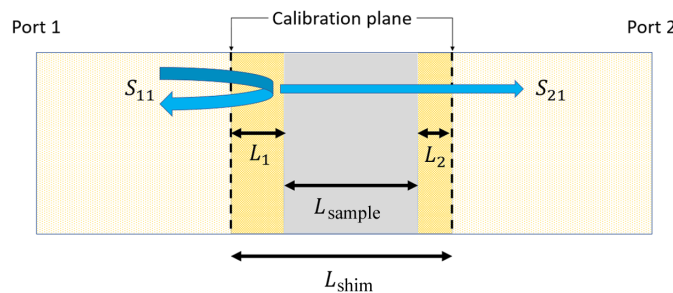


**Fig. 1** Diagram for the measurement of a dielectric sample in a rectangular waveguide.  $L_1$  and  $L_2$  can be positive (sample interface farther from a port relative to the reference plane) or negative (closer to the port).  $S_{12}$  and  $S_{22}$  are not depicted for clarity.

$$R_1 = \exp(-\gamma_0 L_1), \quad (8)$$

$$R_2 = \exp(-\gamma_0 L_2), \quad (9)$$

where  $\gamma_0$  and  $\gamma$  represent the wave propagation constants of the empty and sample-filled waveguides, respectively,  $L_{\text{sample}}$  is the sample thickness,  $\epsilon_r$  is the relative permittivity of the sample,  $L_1$  and  $L_2$  are the distances between the calibration planes and the sample surfaces,  $\kappa_0$  is the wavenumber in free space ( $\kappa_0 = \omega/c$ ), and  $\kappa_c$  is the cutoff wavenumber of the TE<sub>10</sub> (dominant) mode, given by  $\kappa_c = \pi/a$ , where  $a$  is the width of the waveguide.

The calibration planes are separated by  $L_{\text{shim}}$ , an arbitrary length of waveguide containing the sample of interest, as illustrated in Fig. 1. For a sample of dielectric material with surfaces that are exactly at the reference planes ( $L_{\text{sample}} = L_{\text{shim}}$ ),  $L_1$  and  $L_2$  are zero, leading to  $R_1 = R_2 = 1$  and, subsequently,  $S_{11} = S_{22}$ . This allows Eqs. (1)–(3) to be fit with only the real and imaginary portions of permittivity as free parameters. As an example, Fig. 2 shows the measured and calculated S-parameters for an empty ( $\epsilon_r = 1$ ) section of a waveguide shim, 4.153 mm in length. Both the real and imaginary  $S_{11}/S_{22}$  curves are zero as there is no sample to cause reflections, whereas  $S_{21}/S_{12}$  vary sinusoidally as expected from the propagation phase. The calculated S-parameters are in excellent agreement with the measured data. In the absence of dispersion and sample inhomogeneity, a single real and imaginary permittivity value can be applied to the entire bandwidth of the waveguide measurement system; the entire set of S-parameter data can then be simulated by only two free parameters with no frequency dependence.

In the event that one or both of the sample surfaces are not at the calibration plane,  $L_1$  and  $L_2$  will be non-zero, causing  $R_1$  and/or  $R_2$  to no longer be in unity. This change is observed as a splitting of the  $S_{11}$  and  $S_{22}$  data that is dependent on frequency. Hence,  $L_1$  and  $L_2$  must be accounted for to properly fit the data.<sup>18</sup> Figure 1 illustrates that  $L_1$  and  $L_2$  are positive when the sample surface is farther from the port than the calibration plane. Conversely, when the sample surface sticks out of the shim, thus moving past the reference plane,  $L_1$  and  $L_2$  are negative in sign, and  $L_{\text{sample}}$  becomes larger. The materials of interest are soft putties not machined to fixed dimensions. Samples are prepared by fully packing the waveguide shim, but even careful preparation and handling can lead to sample surfaces not located at the calibration planes. Changes in these surface locations could also result in an incorrect sample thickness, causing an error in the measured permittivity values. Instead of relying on a fixed sample thickness, the distance  $L_{\text{shim}}$  between the calibration planes is used in conjunction with  $L_1$  and  $L_2$  to obtain the sample thickness for calculating permittivity using the relation

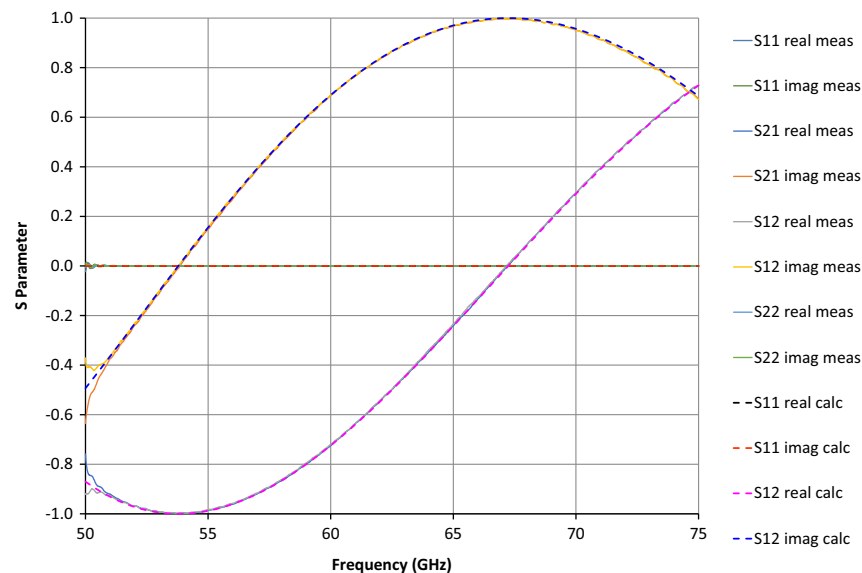


**Fig. 2** Measured (solid) and calculated (dashed) S-parameters for an empty 4.153 mm length V-band shim.  $S_{11}$  and  $S_{22}$  overlap at zero, whereas  $S_{21}$  and  $S_{12}$  are symmetric and vary sinusoidally.

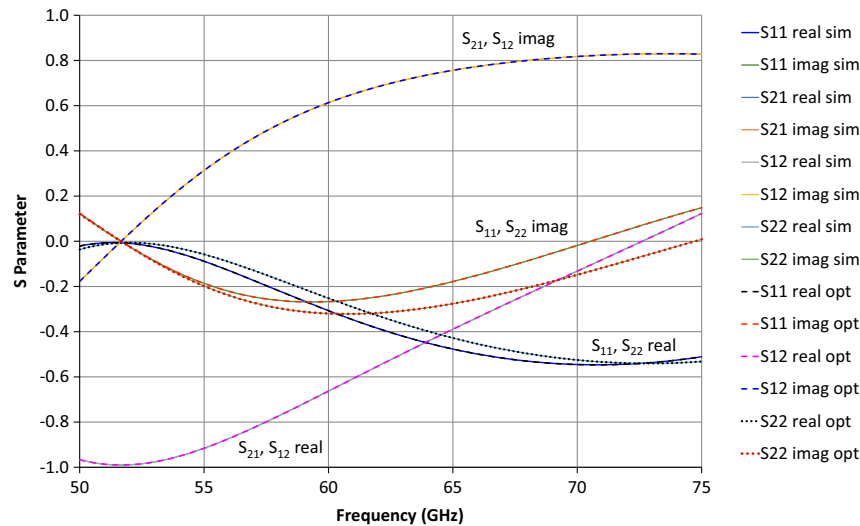


**Fig. 3** Illustration of the effect on the S-parameters caused by a 0.05 mm shift in the sample location, leading to a splitting of  $S_{11}$  and  $S_{22}$  data. Parameters for the simulation were  $\epsilon_r = 2.7 - 0.01i$ ,  $L_{\text{sample}} = L_{\text{shim}} = 2$  mm,  $L_1 = +0.05$  mm,  $L_2 = -0.05$  mm. Solid lines represent simulated data and dashed/dotted lines represent optimized fits of the data.

$$L_{\text{sample}} = L_{\text{shim}} - L_1 - L_2. \quad (10)$$

Figure 3 shows an example of the effect on S-parameters produced by a shift in the sample location. Plastic explosives are weakly absorbing and typically have low permittivity at microwave frequencies,<sup>19</sup> so a value  $\epsilon_r = 2.7 - 0.01i$  is adopted *a priori* for this simulation and will be seen later to be representative of measurements at V-band. The simulated S-parameters (solid lines) are for a 2 mm thick sample contained in a 2 mm shim in which the sample has been shifted toward port 2 by 0.05 mm.  $L_1$  is now +0.05 mm, and  $L_2$  is now -0.05 mm. The shift in the sample with respect to the calibration planes causes a splitting of the  $S_{11}$  and  $S_{22}$  real and imaginary data that varies with frequency. The addition of  $L_1$  and  $L_2$  brings the total of free parameters to four but allows for the effects seen in the simulated S-parameter data to be accounted for.

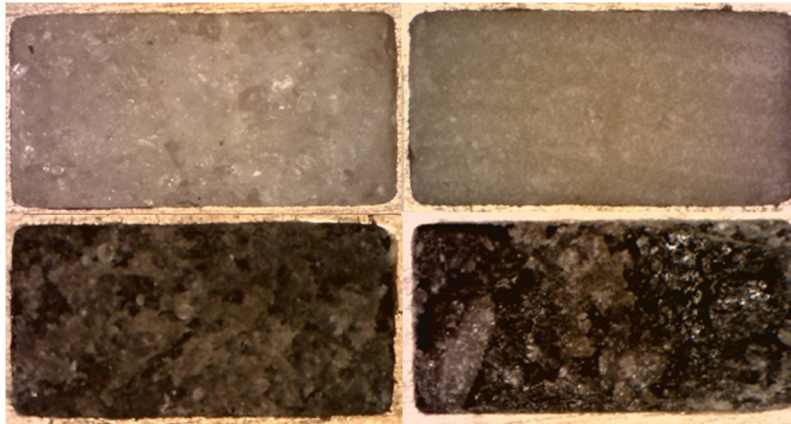
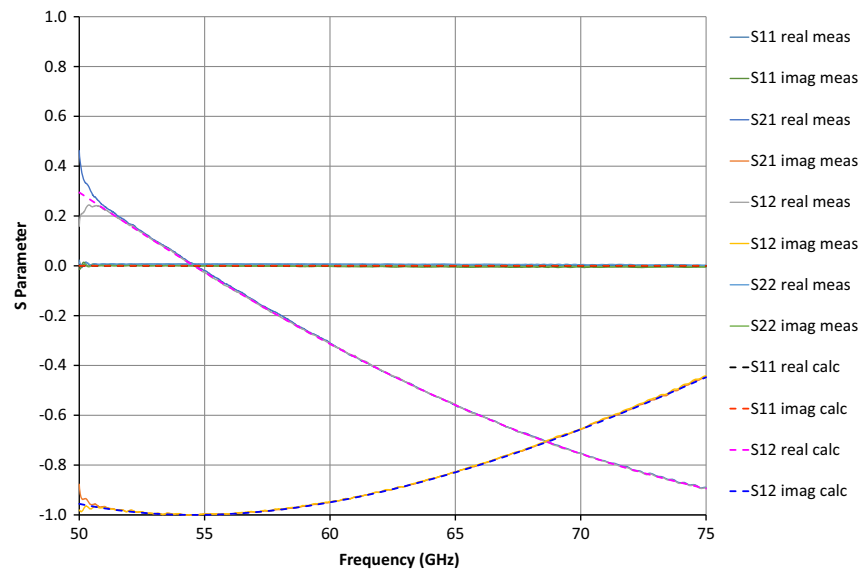
### 3 Experimental Procedure

A Keysight Technologies N5245A PNA-X 50 GHz network analyzer was used in conjunction with two OML Inc. V-band (WR-15) waveguide transceivers operating in the frequency range of 50 to 75 GHz. Data were collected in increments of 10 MHz (2501 points) with an intermediate frequency bandwidth of 3 kHz. The transceivers were calibrated using OML's TRL (thru, reflect, line) calibration kit with measurements of shorts on both ports, a null thru, plus a null  $+1/4 \lambda$  thru. A (nominally) 2 mm length shim obtained from Pasternack Enterprises Inc. was used as the sample holder, with a sample volume of 14 microliters (3.76 mm  $\times$  1.88 mm  $\times$  2 mm). A series of 1- and 2-port measurements, 24 in total, were performed on the 2 mm shim to determine the value of  $L_{\text{shim}}$ . The shim thickness was optimized to the data using Eqs. (1)–(3), using length as the only free parameter.

Table 1 contains the explosives investigated in this work. Samples were manually packed into the waveguide shim, with care taken to pack as uniformly, and as completely, as possible. A plastic spatula was used to trim excess material from the faces of the shim, bringing the sample as close to the shim thickness as possible to minimize  $L_1$  and  $L_2$ . Figure 4 contains representative images of samples packed into the waveguide shim. The sample shim was inserted between the OML transceivers, and a two-port measurement was performed. Five measurements were performed, with the waveguide shim emptied and repacked after each measurement from different parts of the sample to obtain statistical variability. Experimental data were imported into MATLAB and fit to Eqs. (1)–(3) using a least squares fitting algorithm with  $\epsilon_r$  (real,  $\epsilon'$ , and imaginary,  $\epsilon''$ ),  $L_1$ , and  $L_2$  as free parameters.

**Table 1** Explosives investigated in this work.

Explosive	Manufacturer
C-4	Accurate energetics
Primasheet 1000	Ensign-Bickford
Primasheet 2000	Ensign-Bickford
Semtex 10	Explosia

**Fig. 4** Images of plastic explosives loaded into a WR-15 waveguide shim from top left clockwise; C-4, Primasheet 1000, Primasheet 2000, and Semtex 10.**Fig. 5** Representative two-port S-parameter data obtained from the empty Pasternack shim nominally 2 mm in thickness. The dashed lines represent the calculated S-parameters using an optimum value of 2.011 mm for this single measurement.

#### 4 Quality Control of Waveguide SHIMS

Figure 5 shows a representative two-port S-parameter data (solid lines) of the empty Pasternack 2 mm shim along with calculated S-parameters (dashed lines). Because the shim is empty,  $S_{11} = S_{22}$  and  $S_{12} = S_{21}$ . Excellent agreement of the calculated and measured data is obtained using an

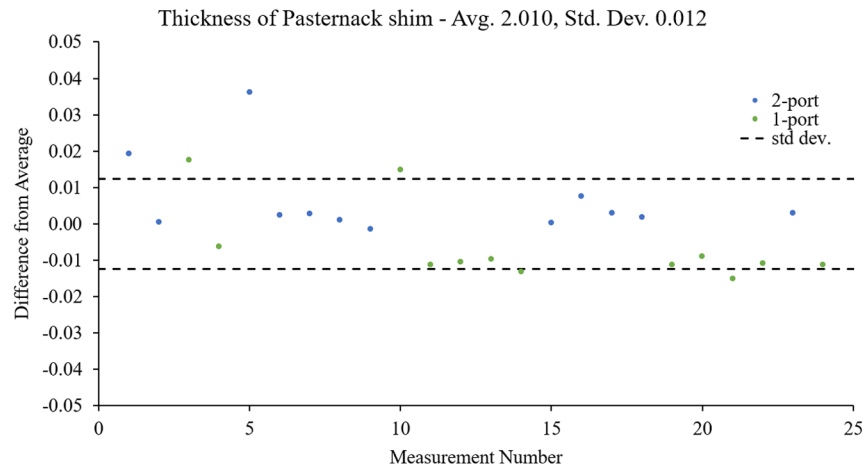


**Fig. 6** Results obtained on 24 measurements of the empty sample shim using two-port and one-port (short backed) measurements.  $L_{\text{shim}}$  was determined to be  $2.01 \pm 0.01$  mm.

optimum value of 2.011 mm as the only free parameter. Figure 6 plots the optimum thickness values obtained from 24 total 2-port (transmission/reflection) and 1-port (short-backed reflection-only) measurements on the empty shim. The empty shim resulted in a length value of  $2.010 \pm 0.012$  mm for the shim, which is consistent both with the length  $2.00 \pm 0.02$  mm measured with a Mitutoyo 500-197-20 digital caliper and the  $\pm 0.02$  mm accuracy specified by the shim manufacturer. The average value 2.010 mm was used for  $L_{\text{shim}}$  for all analysis samples. Scatter in the data is likely indicative of the repeatability of the connections at the waveguide interfaces. The results obtained from analysis of the separate two-port and one-port measurements show that they are not statistically different.

Additional waveguide shims were examined as part of this effort. It was determined that some parts did not conform to expectations from standard waveguide equations. Figure 7 shows representative S-parameter data on a 5 mm V-band shim from an external supplier. Despite optimizing the thickness, poor agreement is obtained between the calculated and measured data. An empty shim should produce no reflections ( $S_{11} = S_{22} = 0$ ), yet signal is observed. Further investigation was performed. Figure 8 presents images obtained with an optical microscope on the 2 mm shim used for data collection in this work [Fig. 8(a) left] and a 5 mm shim from another

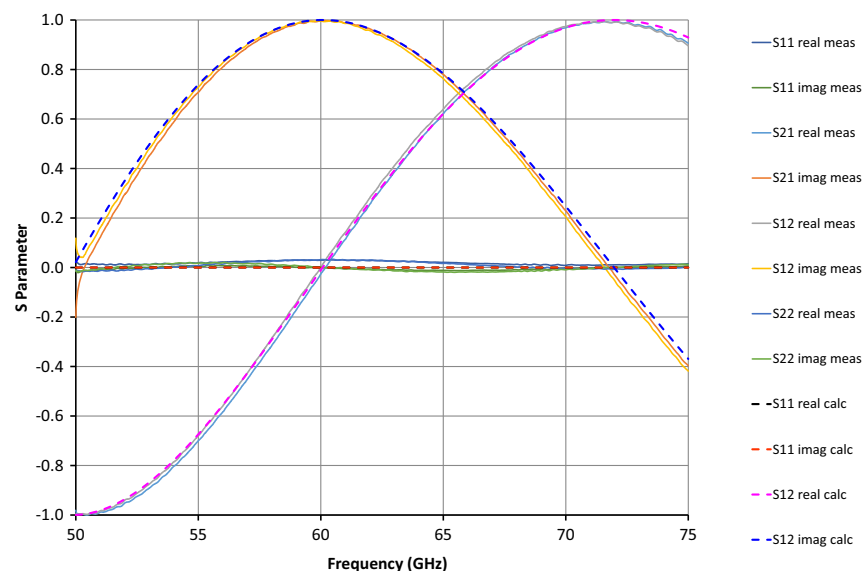


**Fig. 7** Representative two-port S-parameter data obtained from the empty nominally 5 mm shim obtained from a waveguide manufacturer. Poor agreement is obtained between the calculated and measured data.  $S_{11}$  and  $S_{22}$  values are zero for an ideal empty waveguide.

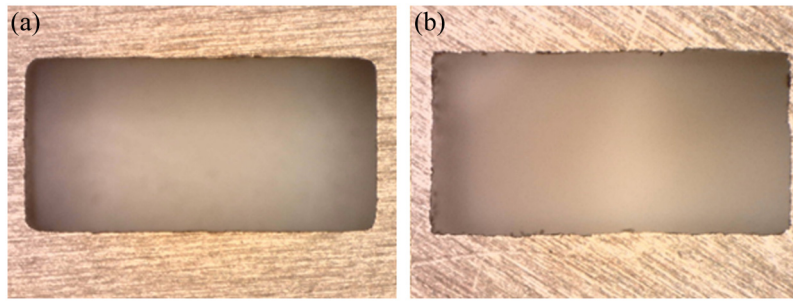


**Fig. 8** Microscope images of V-band shim used for measurements in this work (a) versus another manufacturer (b). Note the poor uniformity of the machining of the walls and corners. The shim on the right was rejected for use in dielectric measurements.

supplier [Fig. 8(b) right]. The walls and corners of the shim on the right are poorly formed, leading to the data obtained in Fig. 7. As a result of this investigation, this shim was rejected for use in the laboratory. A general rule for the acceptability of the experimental setup can be defined from the reflection coefficient of the shim. The  $S_{11}$  reflection coefficient from the rejected shim was 0.1 or  $-20$  dB. The rule requires that the reflection from the shim be less than 10% of the reflection coefficient being measured. For a reflection coefficient of 0.14, the reflection from the shim can be specified to be less than 0.014 or  $-37$  dB, to avoid the problems evident in Fig. 7.

## 5 Results of Dielectric Measurements

A representative set of two-port S-parameters obtained from a sample of C-4 is presented in Fig. 9. Measured data are presented as solid lines, and calculated data are shown in dashed/dotted lines. Optimizing the scattering functions with the four free parameters— $\epsilon'$ ,  $\epsilon''$ ,  $L_1$ , and  $L_2$ —yields excellent agreement of the calculated S-parameters to the measured data. The optimized values from this measurement (measurement 1) and four others are presented in Table 2. From the five measurements, C-4 is determined to have an average permittivity value of  $\epsilon_r = 3.19(5) - 0.029(3)i$ ; the uncertainties in the last digits are given in parentheses. Uncertainty values were calculated from the standard deviation of the measurements and uncertainty in the thickness of the sample shim. This procedure was repeated for Primasheet 1000, Primasheet 2000, and Semtex 10. Table 3 provides the results obtained for all four explosives

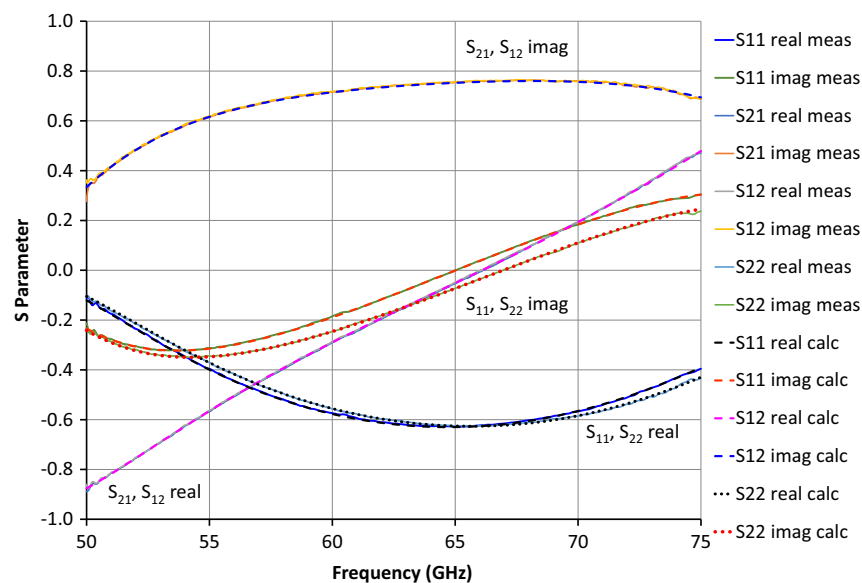


**Fig. 9** 2-port S-parameter measured and calculated data for a sample of C-4 packed in the 2 mm waveguide shim. Optimized values for  $\epsilon_r$ ,  $L_1$ , and  $L_2$  for this data are listed in Table 2 under measurement 1. The calculated S-parameters are in excellent agreement with the measurement.

**Table 2** Results of dielectric measurements for samples of C-4. Real and imaginary permittivity,  $L_1$  and  $L_2$ , are optimized;  $L_{\text{sample}}$  is determined using Eq. (10), and  $L_{\text{shim}} = 2.010$  mm.

Measurement	$\epsilon'$	$\epsilon''$	$L_1$ (mm)	$L_2$ (mm)	$L_{\text{sample}}$ (mm)
1	3.240	0.028	0.030	-0.023	2.003
2	3.218	0.030	0.102	0.068	1.840
3	3.163	0.033	0.195	-0.067	1.882
4	3.157	0.028	0.045	0.089	1.876
5	3.197	0.027	-0.003	0.062	1.952
Average	3.19	0.029			
Std. Dev.	0.04	0.002			

**Table 3** Compilation of plastic explosive dielectric data as a function of frequency. The uncertainties in the last digits are given in parentheses.

Material	Frequency (GHz)	$\epsilon'$	$\epsilon''$	Technique	Source
C-4	50 to 75	3.19(5)	0.029(3)	Loaded waveguide	This work
C-4	75	3.28	0.008	THz-TDS	20
C-4	50 to 100	3.1	0 to 0.2	Quasioptical	21
Primasheet 1000	50 to 75	2.83(4)	0.061(2)	Loaded waveguide	This work
Primasheet 1000	60 to 90	2.99(7)	0.086(7)	Free space reflectometry	10
Primasheet 1000	18 to 40	2.86(2)	0.105(7)	Free space reflectometry	22
Primasheet 2000	50 to 75	3.19(7)	0.021(2)	Loaded waveguide	This work
Semtex 10	50 to 75	2.84(5)	0.048(3)	Loaded waveguide	This work

studied in this work along with data on C-4 and Primasheet 1000 available in the literature. Results obtained for C-4 and Primasheet 1000 in this work are comparable to the literature values, providing confidence in the results. It is also noted that, as manufactured products, samples of plastic explosives can be subject to variations in formulation and uniformity that could account for the slight differences in measured permittivity values.

## 6 Conclusions

Complex permittivity values for C-4, Primasheet 1000, Primasheet 2000, and Semtex 10 in the operating frequency of 50 to 75 GHz were obtained. Excellent agreement between this experiment and the fit was obtained using a constant permittivity across the waveguide band, indicating that dispersion was not significant for these materials. Permittivity values for C-4 and Primasheet 1000 were comparable to values reported in the literature in the millimeter wave (MW) range; the data on Primasheet 2000 and Semtex 10 are the first known published permittivity values in this range.

## Disclosures

The authors affirm that there are no conflicts of interest with this work.

## Code and Data Availability

The datasets used and analyzed in the current study are publicly available in the Zenodo repository at <https://zenodo.org/records/10213766>.<sup>23</sup> The Isqcurvefit function in MATLAB version 2019a was used to fit the data using the theory presented in the paper.

## Acknowledgments

This study was funded by the U.S. Department of Homeland Security (DHS) Science and Technology Directorate (S&T). Battelle/MAG Aerospace were supported under DHS (Grant No. 70RSAT19FR0000136). The views and conclusions contained in this document are those of the authors and should not be interpreted as representing the official policies, either expressed or implied, of the DHS S&T or the U.S. Government. The U.S. Government is authorized to reproduce and distribute reprints for Government purposes not withstanding any copyright notation herein. References or images herein to any specific commercial products, processes, equipment, or services do not constitute or imply its endorsement, recommendation, or favoring by the U.S. Government or DHS, or any of its employees or contractors. This paper was presented at a conference: Z. J. Landicini, J. Barber, J. C. Weatherall, D.C. Karns, P.R. Smith, J. Aparicio-Bolano, and W. Ruiz, "Loaded waveguide measurements of plastic explosives at V-band," *Proc. SPIE*, vol. 12535, pp. 156-166, 2023.

## References

1. D. Karns et al., "Simulant development of a powder explosive material for a millimeter wave imaging system using a resonant cavity with ensemble averaging and the Houston criterion," *Proc. SPIE* **11745**, 117450K (2021).
2. C. Richard et al., "A protocol for simulant validation using active millimeter-wave imaging systems," *Proc. SPIE* **11411**, 114110A (2020).
3. D. Karns et al., "Simulant development for liquid explosive materials using millimeter wavelength characterization and ensemble averaging," *Proc. SPIE* **11411**, 1141109 (2020).
4. J. C. Weatherall et al., "Suitability of explosive simulants for millimeter-wave imaging detection systems," *Proc. SPIE* **10994**, 109940G (2019).
5. J. Barber et al., "Millimeter wave measurements of explosives and simulants," *Proc. SPIE* **7670**, 76700E (2010).
6. Rohde & Schwarz GmbH & Co., "QPS quick personnel security scanners," PD 3606.7160.12 Version 05.00, 2022, [www.rohde-schwarz.com/securityscanner](http://www.rohde-schwarz.com/securityscanner) (accessed 26 Sept. 2023).
7. S. S. Ahmed, A. Schiessl, and L. P. Schmidt, "A novel fully electronic active real-time imager based on a planar multistatic sparse array," *IEEE Trans. Microwave Theory Tech.* **59**, 3567–3576 (2011).
8. S. S. Ahmed et al., "Advanced microwave imaging," *IEEE Microwave Mag.* **13**, 26–43 (2012).
9. A. Schiessl, S. S. Ahmed, and L.-P. Schmidt, "Motion effects in multistatic millimeter-wave imaging systems," *Proc. SPIE* **8900**, 890007 (2013).
10. P. R. Smith et al., "Measurements of the dielectric properties of explosives and inert materials at millimeter wave frequencies (V-band and above) using free space reflection methods," *Proc. SPIE* **10189**, 1018908 (2017).
11. N. Reyes et al., "Complex dielectric permittivity of engineering and 3D-printing polymers at Q-band," *J. Infrared, Millimeter, Terahertz Waves* **39**, 1140–1147 (2018).
12. J. Baker-Jarvis, E. J. Vanzura, and W. A. Kissick, "Improved technique for determining complex permittivity with the transmission/reflection method," *IEEE Trans. Microwave Theory Tech.* **38**, 1096–1103 (1990).
13. S. Kim, J. Surek, and J. Baker-Jarvis, "Electromagnetic metrology on concrete and corrosion," *J. Res. Natl. Inst. Stand. and Technol.* **116**, 655 (2011).
14. K. J. Bois et al., "Dielectric plug-loaded two-port transmission line measurement technique for dielectric property characterization of granular and liquid materials," *IEEE Trans. Instrum. Meas.* **48**, 1141–1148 (1999).
15. J. Hunger et al., "Precision waveguide system for measurement of complex permittivity of liquids at frequencies from 60 to 90 GHz," *Rev. Sci. Instrum.* **82**, 104703 (2011).
16. ASTM D 5568-22, *Standard Test Method for Measuring Relative Complex Permittivity and Relative Magnetic Permeability of Solid Materials at Microwave Frequencies*, Vol. **10**, ASTM International, West Conshohocken, Pennsylvania (2022).
17. U. C. Hasar and C. R. Westgate, "A broadband and stable method for unique complex permittivity determination of low-loss materials," *IEEE Trans. Microwave Theory Tech.* **57**, 471–477 (2009).
18. C. Yang and H. Huang, "Determination of complex permittivity of low-loss materials from reference-plane invariant transmission/reflection measurements," *IEEE Access* **7**, 131865–131872 (2019).
19. A. L. Higginbotham Duque, W. L. Perry, and C. M. Anderson-Cook, "Complex microwave permittivity of secondary high explosives," *Propell. Explos. Pyrotech.* **39**, 275–283 (2014).
20. K. Yamamoto et al., "Noninvasive inspection of C-4 Explosive in Mails by Terahertz Time-Domain Spectroscopy," *Jpn. J. Appl. Phys., Part 2* **43**, L414–L417 (2004).
21. E. Sáenz et al., "Sub-millimetre wave material characterization," in *Proc. 5th Eur. Conf. Antennas and Propag. (EUCAP)*, pp. 3183–3187 (2011).

22. J. C. Weatherall, J. Barber, and B. T. Smith, "Spectral signatures for identifying explosives with wideband millimeter-wave illumination," *IEEE Trans. Microwave Theory Tech.* **64**, 999–1005 (2016).
23. EMXLAB DHS/S&T/TSL, "Loaded waveguide measurements of plastic explosives at v-band," Zenodo (2023).

**Zachary J. Landicini** is a scientist for the Battelle Memorial Institute, which supports the U.S. Department of Homeland Security Transportation Security Laboratory (TSL) in Egg Harbor Township, New Jersey, United States. He received his BS degree in biochemistry/molecular biology from Stockton University in 2015. Presently, he is pursuing a master of science degree from Rowan University in electrical and computer engineering.

**Jeffrey Barber** received his BS degree in chemistry from Allegheny College in 1998 and his PhD in chemistry from Oregon State University in 2003. His work has included dielectric measurements of explosives, developing inert simulants and image quality tools for active millimeter wave imaging systems, and the quality control of synthesized explosives via infrared and Raman spectroscopy. In addition to co-authoring numerous publications and conference proceedings, he has been awarded 18 US patents.

**James C. Weatherall** supports explosives detection science as a physical scientist in the Applied Research Division of the TSL. He received his BS degree from Caltech and his PhD in plasma physics from the University of Colorado. He is actively developing methods to improve the airport screening process using the response of potential threats to millimeter-waves during screening. Before coming to the TSL, he worked in high-power microwaves and astrophysics.

**Duane C. Karns** is a physical scientist within the ARD division of the TSL. He received his BS degree from Pennsylvania State University and his PhD in electrical and computer engineering from Carnegie Mellon University, where he specialized in near-field optical systems. His work at the TSL involves MMW characterization of material dielectric properties, including explosives and their simulants and the development of synthetic data for MMW and X-ray imaging systems.

**Peter R. Smith** received his BSEE degree from Northeastern University, Boston, Massachusetts, United States, and his dual MSEE degrees from Columbia University, New York, New York, United States. He is an RF research engineer investigating the interaction of millimeter electromagnetic waves and materials for MAG Aerospace/Battelle Memorial Institute as a contractor for the DHS Science and Technology Directorate at the TSL. He enjoys working on knotty technical problems.

**Joaquín Aparicio-Bolaño** received his MS degree in physics from the University of Puerto Rico at Mayagüez and his PhD in chemical physics from the University of Puerto Rico in Río Piedras in 2011. In the same year, he joined ALERT DHS-COE at UPRM. He is currently a staff physicist at the Battelle Memorial Institute. His current research interests at TSL focus on the physical and chemical characterization of high energetic materials.

**Wendy Ruiz** is a test engineer for the Battelle Memorial Institute working in the Electromagnetic Signatures of Explosives Laboratory at the TSL. She received her bachelor of science degree in biochemistry and biology with a pre-med concentration from Rowan University in 2010. She also has a degree in Spanish literature with a concentration in international studies.